Chemical Engineering Journal xxx (xxxx) xxx–xxx

Contents lists available at ScienceDirect

Chemical Engineering Journal

journal homepage: www.elsevier.com/locate/cej

Equilibrium solubility and kinetics of CO_2 absorption in hexamethylenediamine activated aqueous sodium glycinate solvent

Bikash K. Mondal[a], Amar N. Samanta[b,*]

[a] Chemical Engineering Department, National Institute of Technology Durgapur, Durgapur, India
[b] Chemical Engineering Department, Indian Institute of Technology Kharagpur, Kharagpur, India

HIGHLIGHTS

- Measurement of physico-chemical properties of ternary (HMDA + SG + H_2O) solvent.
- Experimental measurement and modelling of CO_2 solubility in aqueous (HMDA + SG).
- Investigation of CO_2 absorption kinetics in aqueous (HMDA + SG).
- Development of rate model based on the zwitterion mechanism.

ARTICLE INFO

Keywords:
CO_2 capture
Hexamethylenediamine
Sodium glycinate
Solubility
Kinetics

ABSTRACT

Equilibrium solubility and absorption kinetics of CO_2 in hexamethylenediamine (HMDA) activated aqueous sodium glycinate (SG) solvent are measured in the temperature range of 313–333 K. For the experimental investigation, HMDA concentration in the solvent is varied in the range of 5–15 mass% keeping total amine concentration at 30 mass%. Solubility data is presented in the form CO_2 loading (mole CO_2 absorbed per mole of total amine). Kinetics of CO_2 absorption is evaluated assuming pseudo first order reaction condition. Both solubility and kinetics of CO_2 absorption are found to enhance significantly due to addition of small amount of HMDA in the aqueous SG solvent. CO_2 loading data is correlated using modified Kent-Eisenberg model. For developing kinetic model, overall rate is assumed to be the combined rate contribution of CO_2-HMDA and CO_2-SG reaction system. Based on this concept, a kinetic model is proposed using zwitterion mechanism for both the component reaction system. Kinetic and solubility models developed in this work are in good agreement with the experimental data with average absolute deviation of 7.4% and 4.5% respectively.

1. Introduction

One of the most serious problems facing the world today is global warming and consequential climate change. Prevention of the catastrophic global worming requires an effective implementation of CO_2 capture strategy to the major point sources of CO_2 emission. Among the major point sources, fossil fuel-based power plants contribute almost 40% of the anthropogenic discharge. So, the main target for implementing the CO_2 emission-reducing strategy is pointed towards this sector. Aqueous amine-based absorption-regeneration process for capturing CO_2 is a mature technology. Monoethanolamine (MEA), diethanolamine (DEA) are some of the conventional solvents used for rapid capture of CO_2 [1]. But, CO_2 capture from atmospheric pressure flue gas presents a unique set of difficulties due to low CO_2 concentration (10–15 vol.% CO_2) in the flue gas stream and large volumetric flow rate of the flue gas with the considerable amount of oxygen content [2] which are not usually experienced in more conventional gas treating. As a result, implementation of the conventional amine solvent for capturing CO_2 from the power plant flue gas streams leads to high energy requirement, large solvent circulation rate and high solvent degradation rate, all of which in turn increases the operating and capital cost of the carbon capture. These drawbacks of conventional solvents are the main motivation for the investigation of the alternative solvents. An efficient solvent should have high CO_2 absorption rate and capacity, resistant to the thermal and oxidative degradation, low regeneration energy requirement. In this work, CO_2 absorption property of hexamethylenediamine (HMDA) activated aqueous sodium glycinate (SG) solvent is investigated to explore its potential as an efficient alternative solvent for CO_2 capture from power plant flue gas. The ionic nature of aqueous SG makes it more resistant to oxidative (already oxidized to an

* Corresponding author at: Department of Chemical Engineering, Indian Institute of Technology Kharagpur, Kharagpur 721302, India.
E-mail address: amar@che.iitkgp.ernet.in (A.N. Samanta).

https://doi.org/10.1016/j.cej.2019.04.042

acid) and thermal degradation (small stable molecule) which is a desired property for the CO_2 capture from the oxygen rich power plant flue gas. It also provides certain other desirable physical properties such as low volatility and higher surface tension of the solvent [3]. Low regeneration energy requirement for aqueous SG is reported by Salazar et al. [4]. Their work showed that at 323.15 K, CO_2 absorption enthalpy (limiting value at infinite dilution) for 10mass% SG is only 59.5 kJ/mole which is much less than that of MEA. CO_2 absorption capacity of aqueous SG [5–7] is comparable to that of MEA solvent but absorption kinetics [8] of this solvent with CO_2 is not very promising. On the other, HMDA, a straight chain diamine can potentially enhance the absorption properties of the solvent because of its high kinetic [9,10] and absorption capacity [11,12]. All these characteristics of the component solvents motivated us to investigate aqueous (HMDA + SG) hybrid solvent.

2. Experimental

2.1. Materials

Reagent grade HMDA (> 98% pure) and SG (> 99% pure) are purchased from Sigma Aldrich India. No further purification of the chemicals was done before use. Nitrogen (> 99.99% pure) and carbon dioxide (> 99.99% pure) are procured from Linde India Limited. Detail specification of the chemicals used are given in the table below (See Table 1). For preparing aqueous solvent degassed double distilled water is used.

2.2. Density and viscosity

The Density (ρ_{Am}) and viscosity (η_{Am}) are two important physical properties of the aqueous amine solvent. Density data is required for the calculation of the dynamic viscosity data from the kinematic viscosity. Viscosity data is required for estimating pumping energy cost in a gas treating unit. In this work, it is also used to calculate diffusion coefficient of CO_2 in the formulated solution. The density of aqueous solvent is measured using 25×10^{-6} m^3 (at 298 K) Standard Gay-Lussac pycnometer. Kinematic viscosity is measured using Cannon-Fenske viscometer (viscometer constant: 0.004 cSt/s) and then converted to dynamic viscosity using the following expression.

$$\eta_{Am}/cP = (\rho_{Am}/gml^{-1}) \times (\nu_{Am}/cSt) \quad (1)$$

2.3. Nitrous oxide (N_2O) solubility and liquid phase mass transfer coefficient

Physical solubility and liquid phase mass transfer coefficient (k_L) for CO_2 absorption in aqueous (HMDA + SG) is estimated indirectly using N_2O analogy because of the reactive interaction of CO_2 with the solvent [13,14]. Due to similar molecular configuration and electronic structure of N_2O as CO_2 and non-reactive characteristics of N_2O with aqueous amine, it is used to estimate physical CO_2 solubility from N_2O solubility data using a proportionality relation called N_2O analogy.

Table 1
Specifications and source of chemicals.

Chemicals	Structure	Source	Purity
Hexamethylenediamine	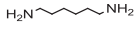	Sigma Aldrich India	0.98 (mass fraction)
Sodium Glycinate	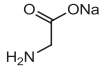	Sigma Aldrich India	0.99 (mass fraction)
Carbon dioxide		Linde India Limited	0.99 (mole fraction)
Nitrogen		Linde India Limited	0.99 (mole fraction)

2.3.1. Experimental set-up and procedure:

Solubility of N_2O and k_L in aqueous (HMDA + SG) are measured using a stirred cell contactor as shown in Fig. 1. Details of the experimental set-up and procedure can be found in our previous works [9,15]. Here it is described briefly.

For each experiment, 200 g of solvent is taken in the stirred cell under vacuum condition and heated to the desired temperature. Then, a batch of N_2O gas from the buffer vessel heated to the experimental temperature is fed to the stirred cell to increase the cell pressure slightly above 100 kPa. Due to physical absorption total pressure inside the cell decrease until an equilibrium condition is reached when stirred cell pressure becomes constant. Pressure and temperature of stirred cell and buffer vessel are monitored and logged using a data acquisition system (Kistock, KT-210 model, France).

2.3.2. Equilibrium N_2O solubility

For the estimation of N_2O solubility, method of Versteeg and van Swaaij [13] is used. Physical solubility of N_2O in aqueous amine solution is estimated using the following expression.

$$m_{N_2O} = \frac{RT}{H_{N_2O}} = \frac{(P^i_{N_2O} - P^e_{N_2O})}{P^e_{N_2O}} \cdot \frac{V_g}{V_l} \quad (2)$$

where m_{N_2O} is a dimensionless quantity given by the ratio of the liquid-phase concentration to the gas-phase concentration of the solute at equilibrium condition, H_{N_2O} is Henry Law constant, $P^i_{N_2O}$ is initial N_2O partial pressure in the cell, $P^e_{N_2O}$ is the equilibrium partial pressure of N_2O in the cell, V_g and V_l are gas phase and liquid phase volume in the cell.

2.3.3. Liquid phase mass transfer coefficient (k_L)

Liquid phase mass transfer coefficient (k_L) is estimated from the slope of the $\ln P_{N_2O}$ versus time data, using the following expression [16].

$$\ln P_{N_2O}|_{t=t} = -\frac{m_{N_2O} A k_L}{V_g} t + \ln P_{N_2O}|_{t=0} \quad (3)$$

where V_g and A are the gas phase volume and interfacial area of gas-liquid interaction respectively. P_{N_2O} and m_{N_2O} denote N_2O partial pressure in the stirred cell and dimensionless physical solubility parameter respectively.

2.4. Equilibrium CO_2 solubility

Equilibrium solubility or vapour-liquid equilibrium (VLE) data is important to understand the distribution of the molecular and ionic species between the vapour and liquid phase. VLE data measured in this work is the combined solubility due to physical and chemical absorption.

Details of the experimental set-up and procedure is presented in our earlier works [17,18]. The experimental set-up and procedure are similar to that used for the N_2O solubility measurement (Fig. 1) with the buffer vessel connected with an equilibrium cell (405×10^{-6} m^3).

VLE data in this work is expressed as mole of CO_2 absorbed per mole of total amine (HMDA + SG) at equilibrium condition (CO_2 loading). Method of Park and Sandall [19] is followed to estimate CO_2 loading data as given below.

$$\alpha_{CO_2} = \frac{\text{mole } CO_2 \text{ absorbed in liquid phase } (n^l_{CO_2})}{\text{mole amine initially taken } (n_{am})} = \frac{n^T_{CO_2} - n^g_{CO_2}}{n_{am}}$$
$$= \frac{1}{RT\, n_{am}} \left[V_b \left(\frac{P_{b1}}{Z_1} - \frac{P_{b2}}{Z_2} \right) - \frac{V^g_c P_{CO_2}}{Z_{CO_2}} \right] \quad (4)$$

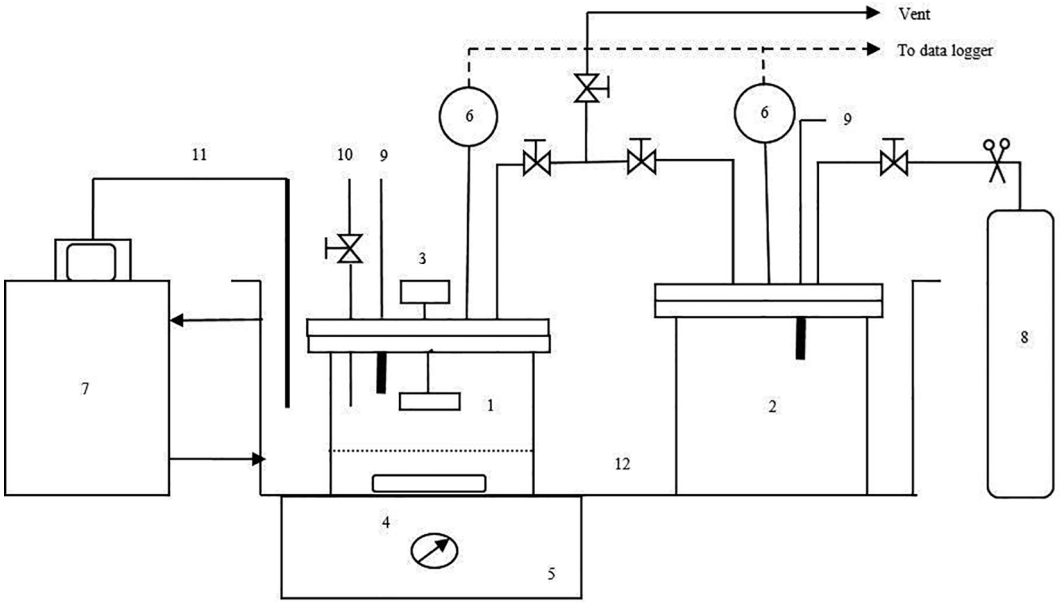

Fig. 1. N_2O solubility measurement setup. [1 – Stirred-cell contactor (500×10^{-6} m^3); 2 – Buffer cell for N_2O storage (650×10^{-6} m^3); 3 – Gas phase stirrer (turbine impeller, Length: 25 mm, Width: 10 mm); 4 – Liquid phase stirrer (Magnetic bar, Dia: 12 mm; Length: 38 mm); 5 – Magnetic stirrer speed controller (REMI 1ML model); 6 – Pressure transducers (Rosemount 3051TA); 7 – Circulator temperature controller (JULABO F32 HL, FRG); 8 – N_2O cylinder; 9 – Temperature sensors (Pt 100); 10 – Liquid solution inlet; 11 – External temperature sensor of circulator temperature controller (Pt 100); 12 – Thermo-stated water bath.]

where V_b is the volume of buffer vessel. P_{b1} and P_{b2} are initial and final buffer pressure. Z_1 and Z_2 are compressibility factors estimated from Peng-Robinson equation of state at temperature T and pressures P_{b1}andP_{b2}, respectively. V_c^g is the gas phase volume of the cell. P_{CO_2} and Z_{CO_2} are equilibrium partial pressure of CO_2 in the cell and corresponding compressibility factor at temperature T, respectively. n_{am} is mole of total amine initially introduced into the cell.

2.5. Kinetics of CO_2 absorption

The knowledge of the kinetics between aqueous amine blend and CO_2 is essential for the evaluation of the mass transfer enhancement due to chemical reaction. The rate of CO_2 absorption in aqueous (HMDA + SG) solution is measured using pressure decay method in a reaction calorimeter (Mettler Toledo, Model: RC1e) set up (Fig. 2). Details of the experimental set-up and procedure are reported in our previous work [9,15]. It is described here briefly.

For kinetic measurement 500 g of solvent is heated in the glass reactor to the desired temperature under vacuum condition. Then, a small amount of CO_2 gas from the feed coil heated to the experimental temperature is transferred to the reactor and pressure decay with time inside the reactor is recorded using data acquisition system (iControl software).

The relation between the pressure inside the reactor and time when operated batch-wise, is given by the following equation [20] which is valid in the pseudo-first-order reaction regime.

$$\ln P_{CO_2}|_{t=t} = -\frac{m_{CO_2}A}{V_g}(\sqrt{k_{ov}D_{CO_2}})t + \ln P_{CO_2}|_{t=0} \quad (5)$$

where V_g and A are the gas phase volume and interfacial area of gas-liquid reaction respectively. P_{CO_2}, m_{CO_2}, D_{CO_2} and k_{ov} denote partial pressure of CO_2, dimensionless physical solubility, diffusivity of CO_2, overall reaction rate constant respectively. From the initial slope of the '$\ln P_{CO_2}$ *versus* t' plot, k_{ov} can be calculated using above equation, since all other inputs are known.

3. Results and discussion

In this work, VLE and kinetics of CO_2 absorption in aqueous (HMDA + SG) hybrid solvent are measured in the temperature e range of 313–333 K. Physico-chemical properties (density, viscosity and physical solubility) which are required to analyse the kinetic data are also measured in the temperature range of 303–333 K. Detail results obtained from different property measurement are as follows.

3.1. Density

Density of aqueous (HMDA + SG) is measured for five compositions with HMDA concentration in the range of 5–25 mass% keeping total (HMDA + SG) concentration 30 mass%. Measured density data at different composition and temperature are given in Table 2 and shown in Fig. 3. As seen from the figure, the density of the solvent linearly decreases with the temperature. Also, density of the solvent decreases with increase in the HMDA concentration in the solvent. This density data is used for the estimation of molar concentration and dynamic viscosity of the solvent.

The density data of this mixed solvent system is correlated using the following empirical expression as a function of temperature and component amine molar concentration.

$$A = a_1 + a_2C_{SG} + a_3C_{HMDA}$$
$$B = b_1 + b_2C_{SG} + b_3C_{HMDA}$$
$$C = c_1 + c_2C_{SG} + c_3C_{HMDA}$$
$$\rho^{Mod} = A + \frac{B}{C+T} \quad (6)$$

where ρ^{Mod} is the predicted density of the solvent in g/ml, T is the temperature in K, C_{SG} and C_{HMDA} are molar concentration of SG and HMDA respectively. Model parameters (a_1, a_2, a_3, b_1, b_2, b_3, c_1, c_2, c_3) are regressed to fit the experimental data with the above expression using least square method. Regressed model parameters are presented in Table 3. Experimental density data of aqueous (HMDA + SG) are compared with the model predicted results in Fig. 3. The figure shows that the developed empirical expression predicts the density data of the

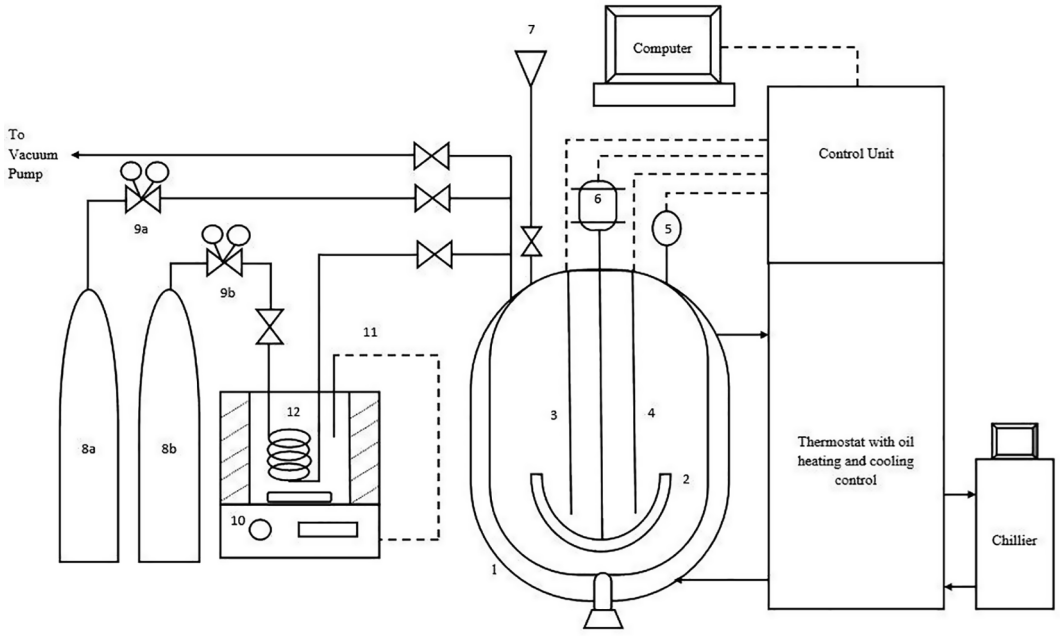

Fig. 2. Schematic of CO_2 absorption rate measurement set up. [1 – Double jacketed glass reactor (Reaction Calorimeter, Model: RC1e; Volume: 1.2×10^{-3} m^3); 2 – Anchor type impeller; 3 – Reactor temperature sensor (Pt 100); 4 – Calibrated heater (25 W); 5 – Pressure transmitter (Rosemount 3051TA Model); 6 – Magnetically coupled stirrer; 7 – Solvent inlet; 8 – (a) N_2 cylinder, (b) CO_2 cylinder; 9 – (a) N_2 gas regulator, (b) CO_2 gas regulator; 10 – Thermo-stated water bath; 11 – Temperature sensor to control water bath temperature; 12 – CO_2 feed coil.]

solvent very well with an average absolute deviation ($AAD = (1/n)\sum_{i=1}^{n} |(M_i^{Exp} - M_i^{Mod})/M_i^{Exp}|$) of 0.03%.

3.2. Viscosity

For the viscosity measurement, same range of aqueous (HMDA + SG) composition are used as that for density measurement. Viscosity data obtained in this work is provided in Table 2 and shown in Fig. 4. As seen from the figure, the dynamic viscosity of the solvent decreases exponentially with temperature. Also, it increases with the increase in the HMDA concentration (mass%) in the in the solvent.

Dynamic viscosity data of the aqueous (HMDA + SG) solvent is correlated using an empirical expression which is assumed to be a function of temperature and molar concentration of the amine components of the solvent. The empirical expression used in this work is given below.

$$A = a_1 + a_2 \ln C_{SG} + a_3 \ln C_{HMDA}$$
$$B = b_1 + b_2 \ln C_{SG} + b_3 \ln C_{HMDA}$$
$$C = c_1 + c_2 \ln C_{SG} + c_3 \ln C_{HMDA}$$
$$\ln \mu^{Mod} = A + \frac{B}{C+T} \quad (7)$$

where μ^{Mod} is predicted dynamic viscosity in cP, T is the temperature in K, C_{SG} and C_{HMDA} are molar concentration of SG and HMDA

Table 2
Physico-chemical properties of aqueous (HMDA + SG).

Composition %SG + %HMDA	Temperature K	Density g/ml	viscosity cP	Diffusivity $\times 10^9$ m^2/s	N_2O Solubility mol/mol	Physical CO_2 solubility mol/mol
5% + 25%	303	0.998	2.592	0.906	–	–
	313	0.992	1.969	1.196	–	–
	323	0.985	1.549	1.538	–	–
	333	0.979	1.246	1.949	–	–
10% + 20%	303	1.026	2.585	0.908	–	–
	313	1.020	1.947	1.207	–	–
	323	1.014	1.541	1.545	–	–
	333	1.007	1.236	1.961	–	–
15% + 15%	303	1.049	2.528	0.923	0.507	0.698
	313	1.044	1.906	1.225	0.439	0.621
	323	1.037	1.524	1.557	0.385	0.557
	333	1.031	1.231	1.968	0.339	0.501
20% + 10%	303	1.078	2.473	0.938	0.482	0.664
	313	1.072	1.890	1.233	0.422	0.596
	323	1.065	1.506	1.571	0.366	0.529
	333	1.058	1.215	1.987	0.321	0.475
25% + 5%	303	1.100	2.398	0.960	0.463	0.638
	313	1.095	1.817	1.270	0.398	0.563
	323	1.089	1.433	1.629	0.348	0.504
	333	1.083	1.178	2.032	0.300	0.444

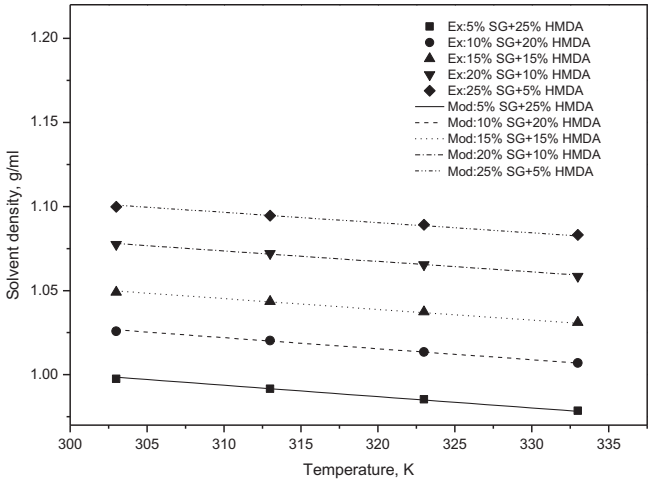

Fig. 3. Density of aqueous (HMDA + SG) solvent: Experimental data and model predictions (AAD: 0.03%).

Table 3
Parameters of the density, viscosity and N_2O solubility model for aqueous (SG + HMDA) solvent.

Parameters	Density model	Viscosity model	N_2O solubility
a_1	−2.023	−6.476	3.539
a_2	0.579	−0.49	3.266
a_3	0.686	−0.691	3.759
b_1	1871.56	2026.27	−285.186
b_2	92.719	341.851	−474.979
b_3	196.983	445.44	−375.957
c_1	196.53	−28.14	1.949
c_2	406.407	26.465	2.047
c_3	534.916	30.461	−12.339

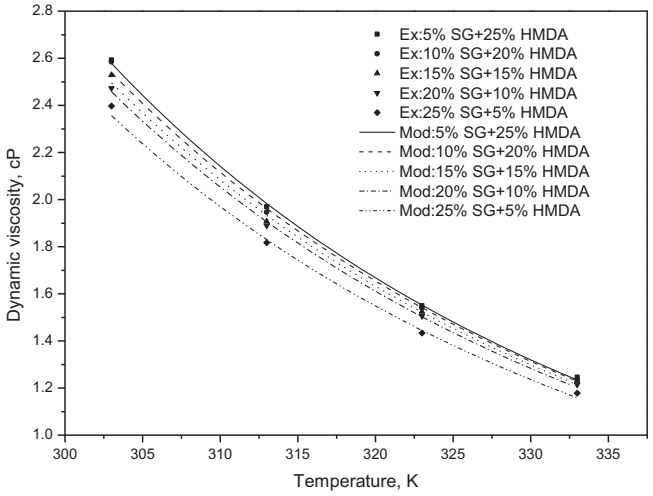

Fig. 4. Viscosity of aqueous (HMDA + SG) solvent: Experimental data and model predictions (AAD: 0.6%).

respectively. Model parameters (a_1, a_2, a_3, b_1, b_2, b_3, c_1, c_2, c_3) are regressed to fit the experimental data with that of the model predicted values. Regressed model parameters are presented in Table 3. For the validation of this model, experimental and model predicted data are compared in Fig. 4. Model prediction shows good agreement with the experimental data with 0.6% deviation (AAD).

Viscosity data measured in this work are used to estimate diffusivity of CO_2 in the mixed solvent at different temperature and solvent composition. It is estimated using modified Stokes-Einstein relation

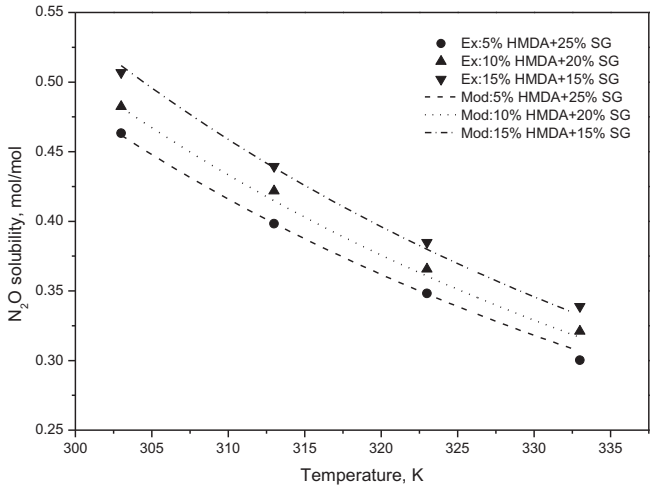

Fig. 5. Nitrous oxide solubility in aqueous (HMDA + SG) solvent: Experimental data and model predictions (AAD: 0.52%).

[10,21] as given shown below.

$$(D_{CO_2,L}.\ \eta^{0.74})|_{water} = (D_{CO_2,L}.\ \eta^{0.74})|_{Am} \tag{8}$$

Diffusivity of CO_2 in water is taken from the work of Versteeg and van Swaaij [13].

$$D_{CO_2,water} = 2.35 \times 10^{-6} \exp\left(\frac{-2119}{T}\right) \tag{9}$$

Estimated diffusivity values are presented in Table 2.

3.3. Physical solubility

For the measurement of N_2O solubility (m_{N_2O}) compositions used in this work are aqueous (5%HMDA + 25% SG), (10% HMDA + 20% SG), and (15% HMDA + 15% SG). Measured solubility data are given in Table 2 and shown in Fig. 5. It is seen from the figure that m_{N_2O} decreases exponentially with the increase in temperature, whereas it increases with the increase in HMDA concentration in the solvent. Experimentally measured N_2O solubility data is then utilized for the estimation of physical CO_2 solubility using N_2O analogy expression as given below [13,14].

$$\left(\frac{m_{CO_2}}{m_{N_2O}}\right)|_{\text{amine solution}} = \left(\frac{m_{CO_2}}{m_{N_2O}}\right)|_{water} \tag{10}$$

To correlate the physical N_2O solubility in aqueous (HMDA + SG) solvent the following empirical equation is used. The functional form of the expression is as follows.

$$\begin{aligned} A &= a_1 + a_2 C_{SG} + a_3 C_{HMDA} \\ B &= b_1 + b_2 C_{SG} + b_3 C_{HMDA} \\ C &= c_1 + c_2 C_{SG} + c_3 C_{HMDA} \\ \ln H_{N_2O}^{Mod} &= A + \frac{B}{C+T} \end{aligned} \tag{11}$$

where $H_{N_2O}^{Mod}$ is predicted Henry coefficient in $m^3kPa.kmol^{-1}$, T is the temperature in K, C_{SG} and C_{HMDA} are molar concentration of SG and HMDA respectively. Least square optimization technique is used to minimize the error between experimental data and predicted results by regressing the model parameters (a_1, a_2, a_3, b_1, b_2, b_3, c_1, c_2, c_3) which are presented in Table 3. Using this empirical expression, model predicted data (converted to m_{N_2O}) are compared with that of the experimental data in Fig. 5 which shows good agreement between experimental and model predicted values with low average absolute deviation (0.52%).

Table 4
Vapour-liquid equilibrium of CO_2 in aqueous (5 %HMDA + 25% SG).

313 K		323 K		333 K	
P_{CO_2} kPa	α_{CO_2} mole/mole	P_{CO_2} kPa	α_{CO_2} mole/mole	P_{CO_2} kPa	α_{CO_2} mole/mole
1.19	0.456	1.74	0.435	3.11	0.424
3.06	0.517	4.12	0.495	7.82	0.496
13.75	0.612	9.99	0.560	20.44	0.571
41.44	0.679	31.59	0.630	33.26	0.601
58.91	0.701	46.45	0.650	55.00	0.628
72.28	0.716	69.68	0.677	67.27	0.640
88.93	0.731	79.53	0.688	83.24	0.654
104.81	0.744	121.08	0.717	112.61	0.674

Table 5
Vapour-liquid equilibrium of CO_2 in aqueous (10 %HMDA + 20% SG).

313 K		323 K		333 K	
P_{CO_2} kPa	α_{CO_2} mole/mole	P_{CO_2} kPa	α_{CO_2} mole/mole	P_{CO_2} kPa	α_{CO_2} mole/mole
5.14	0.635	3.17	0.595	3.69	0.551
9.33	0.671	18.22	0.681	5.07	0.568
16.82	0.712	35.85	0.732	9.41	0.588
42.75	0.772	53.27	0.758	22.67	0.659
62.75	0.802	72.61	0.780	41.66	0.700
84.34	0.826	91.60	0.799	69.29	0.736
103.02	0.844	114.94	0.817	105.87	0.774

Table 6
Vapour-liquid equilibrium of CO_2 in aqueous (15 %HMDA + 15% SG).

313 K		323 K		333 K	
P_{CO_2} kPa	α_{CO_2} mole/mole	P_{CO_2} kPa	α_{CO_2} mole/mole	P_{CO_2} kPa	α_{CO_2} mole/mole
1.03	0.642	1.01	0.586	2.02	0.579
4.43	0.722	6.85	0.703	12.36	0.680
8.09	0.770	11.85	0.743	23.79	0.725
24.61	0.862	28.26	0.822	37.73	0.763
41.58	0.904	41.57	0.852	49.13	0.790
56.35	0.931	52.69	0.871	66.40	0.818
71.99	0.937	68.25	0.896	78.70	0.832
91.43	0.942	99.68	0.903	91.73	0.847
100.49	0.953			106.30	0.861

3.4. Equilibrium CO_2 loading:

VLE of CO_2 in aqueous (HMDA + SG) is measured in the temperature and CO_2 partial pressure range of 313–333 K and 1–100 kPa respectively. For this study, HMDA concentration in the solvent is varied in the range of 5–15 mass% keeping total (HMDA + SG) concentration 30 mass%. VLE data in term of CO_2 loading (mole CO_2/mole total amine) are given in Tables 4–6. Measured VLE data shows that, CO_2 loading decreases with the increase in temperature because of the exothermic nature of the chemical absorption. Also, loading capacity of the solvent increases as the HMDA concentration in the mixture increases with constant total composition (30 mass%) and temperature.

In Fig. 6, loading capacity of aqueous [5 mass% (0.47 M) HMDA + 25mass% (2.81 M) SG] is compared with that of aqueous 30 mass% (3.46 M) SG [7] and aqueous (0.5 M MEA + 2 M SG) [22] taken from the literature. At 313 K and 20 kPa CO_2 partial pressure, loading capacity is enhanced by 26% for aqueous (5 mass% HMDA + 25 mass% SG) and 66% for (15 mass% HMDA + 15 mass% SG) solvent compared to that of 30 mass% SG alone. This indicate that the addition of small amount of HMDA into aqueous SG solution keeping total amine concentration constant (30 mass%), can enhance the loading capacity of the solvent to a great extent. Fig. 6 also shows the higher loading capacity of aqueous (HMDA + SG) compared to that of aqueous (MEA + SG) solvent.

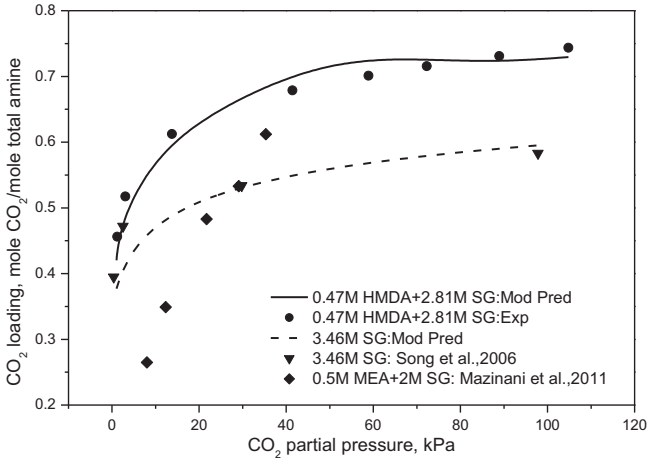

Fig. 6. Comparison of CO_2 loading in aqueous (HMDA + SG) with that of aqueous SG and (MEA + SG) at 313 K.

3.4.1. Kent-Eisenberg model for (H_2O + HMDA + SG + CO_2) system

To correlate vapour-liquid equilibrium of CO_2 in aqueous (HMDA + SG), the vapour phase is considered to be ideal due to moderate experimental pressure range (100 kPa) and the liquid phase is modelled using modified Kent and Eisenberg theory [23–26]. In aqueous medium, phase and chemical equilibrium reactions for (H_2O + HMDA + SG + CO_2) system are as follows.

Physical solubility

$$CO_2(g) \overset{H_{CO_2}}{\leftrightarrow} CO_2(aq) \tag{12a}$$

Water hydrolysis reactions:
Dissociation of bicarbonate ion

$$HCO_3^- \overset{K_1}{\leftrightarrow} CO_3^{2-} + H^+ \tag{12b}$$

Formation of bicarbonate ion

$$CO_2 + H_2O \overset{K_2}{\leftrightarrow} HCO_3^- + H^+ \tag{12c}$$

Ionization of water

$$H_2O \overset{K_3}{\leftrightarrow} OH^- + H^+ \tag{12d}$$

Reactions with HMDA:
Deprotonation of HMDA

$$HMDAH^+ \overset{K_4}{\leftrightarrow} HMDA + H^+ \tag{12e}$$

Formation of mono-carbamate

$$HMDA + CO_2 \overset{K_5}{\leftrightarrow} HMDACOO^- + H^+ \tag{12f}$$

Formation of bicarbamate

$$HMDACOO^- + CO_2 \overset{K_6}{\leftrightarrow} HMDA(COO^-)_2 + H^+ \tag{12g}$$

Reactions with SG:
Amine deprotonation

$$H_3N^+CH_2COO^- \overset{K_7}{\leftrightarrow} NH_2CH_2COO^- + H^+ \tag{12h}$$

Carbamate hydrolysis

$$-OOCCH_2NHCOO^- + H_2O \overset{K_8}{\leftrightarrow} -OOCCH_2NH_2 + HCO_3^- \tag{12i}$$

The phase equilibrium which relates equilibrium CO_2 partial pressure (P_{CO_2}) with the physically dissolved CO_2 concentration ($[CO_2]$) in the liquid phase is governed by Henry's Law as given below.

$$P_{CO_2} = H_{CO_2}[CO_2] \tag{13}$$

The chemical equilibrium is presented by the apparent equilibrium constant based on the chemical species concentration for the above reactions.

$$K_1 = \frac{[CO_3^{2-}][H^+]}{[HCO_3^-]} \tag{14}$$

$$K_2 = \frac{[HCO_3^-][H^+]}{[CO_2]} \tag{15}$$

$$K_3 = [H^+][OH^-] \tag{16}$$

$$K_4 = \frac{[HMDA][H^+]}{[HMDAH^+]} \tag{17}$$

$$K_5 = \frac{[HMDACOO^-][H^+]}{[HMDA][CO_2]} \tag{18}$$

$$K_6 = \frac{[HMDA(COO^-)_2][H^+]}{[HMDA(COO^-)][CO_2]} \tag{19}$$

$$K_7 = \frac{[NH_2CH_2COO^-][H^+]}{[H_3N^+CH_2COO^-]} \tag{20}$$

$$K_8 = \frac{[-OOCCH_2NH_2][HCO_3^-]}{[-OOCCH_2NHCOO^-]} \tag{21}$$

Overall mass balances and charge balance equations can be written as follows

HMDA balance:

$$[HMDA]_t = [HMDA] + [HMDAH^+] + [HMDACOO^-] + [HMDA(COO^-)_2] \tag{22}$$

SG Balance:

$$[SG]_t = [H_2NCH_2COO^-] + [-OOCCH_2NHCOO^-] + [H_3NH^+CH_2COO^-] \tag{23}$$

CO_2 balance:

$$\alpha_{CO_2} \times ([HMDA]_t + [SG]_t) = [CO_2] + [HCO_3^-] + [CO_3^{2-}] + [HMDACOO^-] + 2[HMDA(COO^-)_2] + [-OOCCH_2NHCOO^-] \tag{24}$$

Charge balance:

$$[H^+] + [HMDAH^+] + [Na^+] = [HMDACOO^-] + 2[HMDA(COO^-)_2] + [H_2NCH_2COO^-] + 2[-OOCCH_2NHCOO^-] + [HCO_3^-] + 2[CO_3^{2-}] + [OH^-] \tag{25}$$

where α_{CO_2} is CO_2 loading, $[HMDA]_t$ and $[SG]_t$ are initial molar concentrations of HMDA and SG respectively.

In this work, K_1–K_3 [27], K_4 [28] and K_7 [29] are taken from the literature. Temperature dependency of these equilibrium constants is expressed as shown below.

$$lnK_i = a_i + b_i/T + c_i \ln T \tag{26}$$

where a_i, b_i and c_i are coefficients of the expression which are given in Table 7. The expression for the Henry constants (H_{CO_2}) is taken from the work of Hsu [30] as given below.

$$lnH_{CO_2}(kPa.\ m^3/Kmol) = 20.2669 - \frac{1.38306 \times 10^4}{(T/K)} + \frac{0.06913 \times 10^8}{(T/K)^2} - \frac{0.015589 \times 10^{11}}{(T/K)^3} + \frac{0.012 \times 10^{13}}{(T/K)^4} \tag{27}$$

Table 7
Expression for equilibrium constants used in the Kent-Eisenberg Model of (H_2O + HMDA + SG + CO_2) system.

$\ln K_1 = 220.067 - \frac{12431.7}{T} - 35.4819 \ln T$	[27]
$\ln K_2 = 235.482 - \frac{12092.1}{T} - 36.7816 \ln T$	[27]
$\ln K_3 = 140.932 - \frac{13445.9}{T} - 22.4773 \ln T$	[27]
$\ln K_4 = -1.6664 - \frac{7001.6}{T}$	[28]
$\ln K_7 = -61.6499 + 0.202203\ T - 0.000237956\ T^2$	[29]

3.4.2. Parameter regression & model prediction

Apparent equilibrium constant for carbamate (K_5) and bicarbamate (K_6) formation reaction for HMDA and carbamate hydrolysis (K_8) reaction for SG are regressed as a function of CO_2 loading and temperature to fit the experimental CO_2 loading data with the model expression. Generalized reduced gradient nonlinear optimization technique is used to minimize the error between the experimental and model predicted data. The objective function (F) used in this work is as follows.

$$F = \frac{1}{N}\sum_{i=1}^{N}\left|\frac{\alpha_{CO_2,i}^{Ex} - \alpha_{CO_2,i}^{Mod}}{\alpha_{CO_2,i}^{Ex}}\right| \tag{28}$$

where $\alpha_{CO_2,i}^{Ex}$ and $\alpha_{CO_2,i}^{Mod}$ are experimental and model predicted CO_2 loading data. N is the total number of data points. Along with this objective function the charge balance expression is taken as the constraint function. Regressed equilibrium constants (K_5, K_6 and K_8) expressed in terms of temperature and CO_2 loading are as follows.

$$\ln K_5 = -0.9178 - 1.4025\,\alpha_{CO_2} + \frac{0.9712}{T} - \alpha_{CO_2}^2 + \frac{1.0189}{T^2} + 0.9650\ \frac{\alpha_{CO_2}}{T} \tag{29}$$

$$\ln K_6 = 7.9352 + 7.6220\,\alpha_{CO_2} + \frac{10.008}{T} + 8.0632\alpha_{CO_2}^2 + \frac{10.0046}{T^2} + 9.9981\ \frac{\alpha_{CO_2}}{T} \tag{30}$$

$$\ln K_8 = 13.8067 - 9.3798\,\alpha_{CO_2} - \frac{2378.95}{T} - 14.5356\,\alpha_{CO_2}^2 - \frac{3.4594}{T^2} + 7031.09\frac{\alpha_{CO_2}}{T} \tag{31}$$

Using these equilibrium constants, predicted solubility data is compared with that of the experimentally measured data and are shown in the Figs. 7–9. CO_2 loading in aqueous 30 mass% SG predicted by this

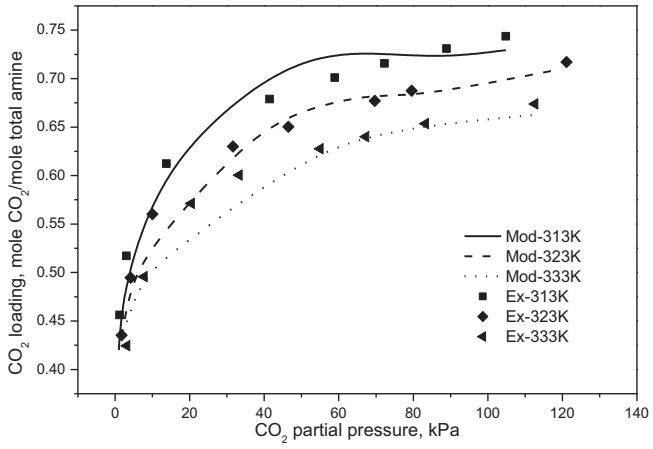

Fig. 7. CO_2 loading in aqueous (5%HMDA + 25%SG): Experimental data and model predictions.

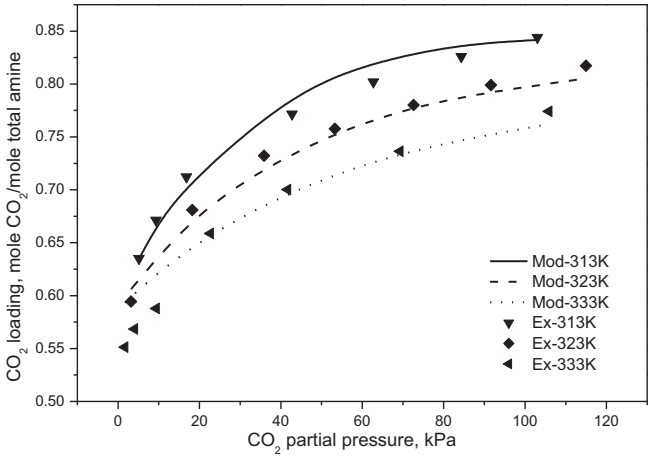

Fig. 8. CO_2 loading in aqueous (10%HMDA + 20%SG): Experimental data and model predictions.

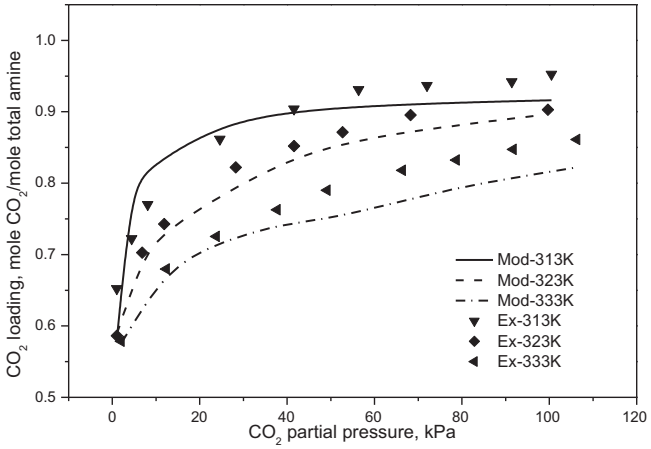

Fig. 9. CO_2 loading in aqueous (15%HMDA + 15%SG): Experimental data and model predictions.

model is also compared with the literature data [7] in Fig. 6. AAD between the experimental data and model predicted results is estimated to be 4.5% considering all the data sets.

3.5. Kinetics of CO_2 absorption

3.5.1. Overall reaction rate constant

The overall rate constant (k_{OV}) for (CO_2 + H_2O + HMDA + SG) system estimated at different temperature and composition are presented in Table 8 and shown in Fig. 10. Reported values of k_{OV} for 30% aqueous SG [8] is also shown in Fig. 10 to compare its CO_2 absorption rate with the formulated solvent. It is seen from the figure that k_{OV} increases with the increase in both temperature and HMDA concentration in the solvent. It also shows that the replacement of small amount of SG with HMDA at constant total amine concentration enhances the CO_2 absorption rate significantly. At 313 K, overall rate constant value for aqueous (5 mass% HMDA + 25 mass% SG) is 5 times higher than that for 30 mass% SG alone. With the increase in the HMDA concentration in the solvent keeping total amine concentration constant (30 mass%) higher rate enhancement is observed.

3.5.2. Kinetic model

For developing kinetic model, overall rate is assumed to be the combined rate contribution of CO_2-HMDA and CO_2-SG reaction system.

3.5.2.1. Reaction rate dependence on SG:. SG is the sodium salt of the primary amino acid, glycine. For the kinetics of CO_2 absorption in aqueous glycinate salt, zwitterion mechanism is used by many authors [3,31–33]. Reaction steps for this system is shown below.

Table 8
Kinetic data for the absorption of CO_2 in aqueous (HMDA + SG).

Concentration mass% HMDA	mass% SG	T K	k_L 10^5 m s^{-1}	k_{OV} s^{-1}	Ha	E_i
5	25	313	2.22	10410.2	164	1206
		323	2.73	15125.0	182	1379
		333	3.30	20801.1	198	1595
10	20	313	2.18	25991.0	259	1074
		323	2.68	34441.0	274	1237
		333	3.23	40869.1	279	1402
15	15	313	2.17	45199.1	343	963
		323	2.63	52665.3	345	1099
		333	3.15	60541.7	348	1242

In this work, we have assumed that the CO_2-SG reaction system will follow a second order reaction rate as indicated by Lee et al. [8].

$$r_{CO_2-SG} = k_{2,SG}[SG][CO_2] \tag{33}$$

3.5.2.2. Reaction rate dependence on HMDA:. The rate contribution of CO_2-HMDA reaction is analysed using zwitterion mechanism. According to this mechanism, the reaction steps and the corresponding rate expression is presented as follows.

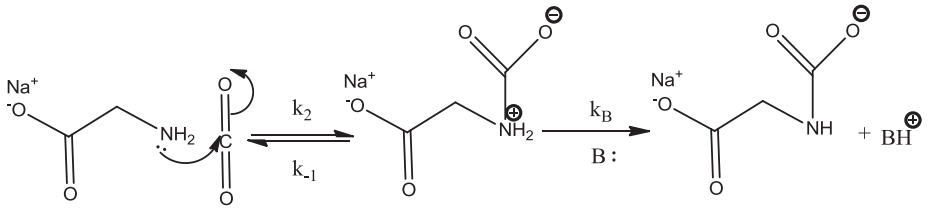

(32)

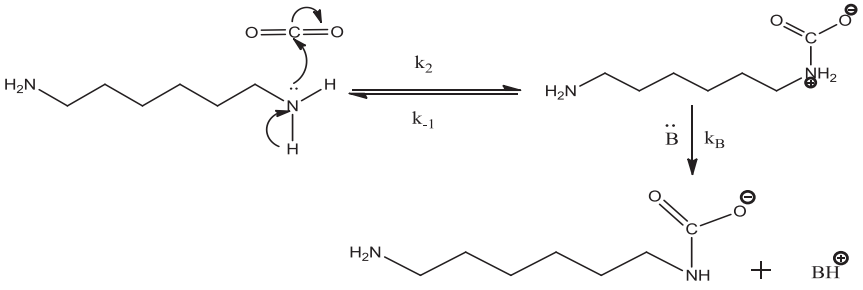

(34)

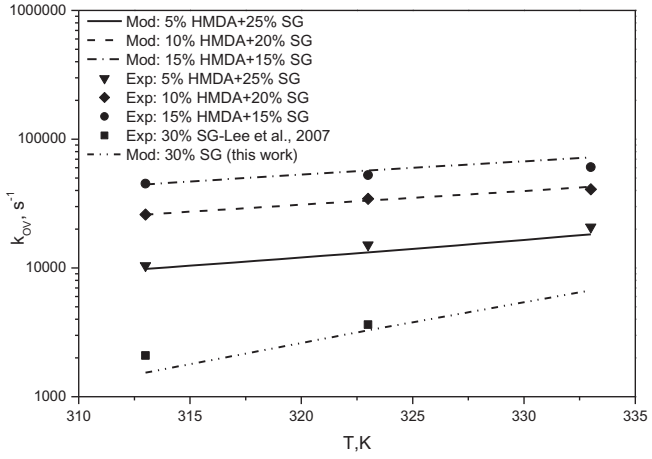

Fig. 10. Overall reaction rate constant for CO_2 absorption in aqueous (HMDA + SG).

$$r_{CO_2-HMDA} = \frac{[HMDA][CO_2]}{\frac{1}{k_{2,HMDA}} + \frac{1}{\frac{k_{2,HMDA}k_{H_2O}}{k_{-1}}[H_2O] + \frac{k_{2,HMDA}k_{SG}}{k_{-1}}[SG] + \frac{k_{2,HMDA}k_{HMDA}}{k_{-1}}[HMDA]}} \quad (35)$$

where $k_{2,HMDA}$ and k_{-1} are the forward and reverse rate constant for the zwitterion formation reaction. k_{H_2O}, k_{SG} and k_{HMDA} are the rate constant for the proton removal reaction from the zwitterion by the bases H_2O, SG, and HMDA respectively. The contribution of OH^- ion is neglected because of low concentration.

3.5.2.3. Reaction rate dependence on water:. Reaction of CO_2 with water can be presented by the following reactions

$$CO_2 + H_2O \leftrightarrow H_2CO_3 \quad (36)$$

$$CO_2 + OH^- \leftrightarrow HCO_3^- \quad (37)$$

Since the rate constant for the CO_2-H_2O reaction is very small ($k_{H_2O} = 0.02\ s^{-1}$ at 298 K) [34], the contribution of this reaction to the overall rate is generally neglected without significant loss of the accuracy in the reaction rate [3]. Again, the contribution of CO_2-OH^- reaction to the overall reaction kinetics is considered negligible due to low concentration of OH^- ion [32].

3.5.2.4. Overall reaction rate of CO_2 with (HMDA + SG + H_2O):. The overall reaction rate for the absorption of CO_2 in aqueous (HMDA + SG) is expressed as shown below.

$$r_{OV} = k_{2,SG}[SG][CO_2] + \frac{[HMDA][CO_2]}{\frac{1}{k_{2,HMDA}} + \frac{1}{\frac{k_{2,HMDA}k_{H_2O}}{k_{-1}}[H_2O] + \frac{k_{2,HMDA}k_{SG}}{k_{-1}}[SG] + \frac{k_{2,HMDA}k_{HMDA}}{k_{-1}}[HMDA]}} \quad (38)$$

$$= k_{OV}[CO_2] \quad (39)$$

where k_{OV} is the overall reaction rate constant for (HMDA + SG + H_2O + CO_2) system and its expression is given by the following expression.

$$k_{OV} = k_{2,SG}[SG] + \frac{[HMDA]}{\frac{1}{k_{2,HMDA}} + \frac{1}{\frac{k_{2,HMDA}k_{H_2O}}{k_{-1}}[H_2O] + \frac{k_{2,HMDA}k_{MDEA}}{k_{-1}}[MDEA] + \frac{k_{2,HMDA}k_{HMDA}}{k_{-1}}[HMDA]}} \quad (40)$$

The kinetic model developed for the (HMDA + SG + H_2O + CO_2) reaction system is the function of kinetic constants $k_{2,HMDA}$, $k_{2,SG}$, $k_{2,HMDA}k_{H_2O}/k_{-1}$, $k_{2,HMDA}k_{HMDA}/k_{-1}$, and $k_{2,HMDA}k_{SG}/k_{-1}$. These kinetic constants are evaluated by fitting the model expression (Eq. (40)) to the experimentally measured k_{OV} data. For fitting the experimental data $k_{2,SG}$ [8] and $k_{2,HMDA}$ [9] are set equal to the following expression taken from the literature.

$$k_{2,SG}/(m^3.\ kmol^{-1}.\ s^{-1}) = 1.95 \times 10^{13} \exp\left(\frac{-7670}{T/K}\right) \quad (41)$$

$$k_{2,HMDA}/(m^3.\ kmol^{-1}.\ s^{-1}) = 2.4 \times 10^{9} \exp\left(\frac{-3321}{T/K}\right) \quad (42)$$

All other kinetic constants are regressed in the form of Arrhenius equation as shown below.

$$\frac{k_{2,HMDA}k_{H_2O}}{k_{-1}}/(m^6.\ kmol^{-2}.\ s^{-1}) = 1.73 \times 10^{2} \exp\left(\frac{-2460}{T/K}\right) \quad (43)$$

$$\frac{k_{2,HMDA}k_{SG}}{k_{-1,HMDA}}/(m^6.\ kmol^{-2}.\ s^{-1}) = 3.18 \times 10^{10} \exp\left(\frac{-5688}{T/K}\right) \quad (44)$$

$$\frac{k_{2,HMDA}k_{HMDA}}{k_{-1}}/(m^6.\ kmol^{-2}.\ s^{-1}) = 3.91 \times 10^{6} \exp\left(\frac{-1339}{T/K}\right) \quad (45)$$

Using these kinetic constants, the model predicted data are compared with the experimental k_{OV} values shown in Fig. 10. In this figure model predicted k_{OV} data for aqueous 30 mass% SG is also compared with the literature data [8]. Kinetic model developed in this work shows good agreement between the predicted and experimental data with low deviation (AAD: 7.4%).

To validate the pseudo-first-order reaction condition Hatta number (Ha) and instantaneous enhancement factor (E_i) are calculated for each experimental run and are presented in Table 8. Estimated data shows that, Ha values are higher than 3, and E_i values are quite higher than the Ha values.

4. Conclusion

HMDA activated aqueous SG solvent is investigated in this work to evaluated its potential application as solvent for CO_2 capture from the power plant flue gas. Equilibrium solubility and kinetics of CO_2 absorption in the formulated solvent is studied in the temperature range of 313–333 K. Density, viscosity and physical solubility of the unloaded

aqueous solvent are also measured to analyse the absorption properties. It is observed from the experimental data that the replacement of small amount of SG by HMDA keeping total amine concentration (mass%) constant has a significant effect on the enhancement of both solubility and kinetics characteristics of the aqueous (HMDA + SG) solvent compared to the aqueous SG solvent. The VLE data in the form of CO_2 loading is correlated using modified Kent-Eisenberg model. CO_2 absorption kinetics in this mixed amine solvent is modelled assuming a second order reaction of CO_2 with SG and a zwitterion mechanism for the reaction of CO_2 with HMDA. For developing the kinetic model, it is also assumed that CO_2 reacts with SG in parallel with the CO_2-HMDA reaction and overall reaction rate of CO_2 with aqueous (HMDA + SG) solvent is the combined rate contribution of CO_2-SG and CO_2-HMDA reaction systems. The VLE and kinetic models developed in this work shows good results with average absolute deviation of 4.5% and 7.4% between the model predictions and experimental data respectively.

References

[1] A.L. Kohl, R.B. Nielsen, Gas Purification, fifth ed., Gulf Publishing Company, Texas, 1997.

[2] D.M. D'Alessandro, B. Smit, J.R. Long, Carbon dioxide capture: prospects for new materials, Angew. Chemie Int. Ed. 49 (2010) 6058–6082, https://doi.org/10.1002/anie.201000431.

[3] P.S. Kumar, J.A. Hogendoorn, G.F. Versteeg, P.H.M. Feron, Kinetics of the reaction of CO_2 with aqueous potassium salt of taurine and glycine, AIChE J. 49 (2003) 203–213, https://doi.org/10.1002/aic.690490118.

[4] V. Salazar, Y. Sánchez-Vicente, C. Pando, J.a.R. Renuncio, A. Cabañas, Enthalpies of absorption of carbon dioxide in aqueous sodium glycinate solutions at temperatures of (313.15 and 323.15) K, J. Chem. Eng. Data. 55 (2010) 1215–1218, https://doi.org/10.1021/je9005954.

[5] B.K. Mondal, S.S. Bandyopadhyay, A.N. Samanta, VLE of CO_2 in aqueous sodium glycinate solution - New data and modeling using Kent-Eisenberg model, Int. J. Greenhouse Gas Control 36 (2015) 153–160, https://doi.org/10.1016/j.ijggc.2015.02.010.

[6] F. Harris, K.A. Kurnia, M.I.A. Mutalib, M. Thanapalan, Solubilities of carbon dioxide and densities of aqueous sodium glycinate solutions before and after CO_2 absorption, J. Chem. Eng. Data. 54 (2009) 144–147, https://doi.org/10.1021/je800672r.

[7] H.-J. Song, S. Lee, S. Maken, J.-J. Park, J.-W. Park, Solubilities of carbon dioxide in aqueous solutions of sodium glycinate, Fluid Phase Equilib. 246 (2006) 1–5, https://doi.org/10.1016/j.fluid.2006.05.012.

[8] S. Lee, H. Song, S. Maken, J. Park, Kinetics of CO_2 absorption in aqueous sodium glycinate solutions, Ind. Eng. Chem. Res. 46 (2007) 1578–1583, https://doi.org/10.1021/ie061270e.

[9] B.K. Mondal, S.S. Bandyopadhyay, A.N. Samanta, Kinetics of CO_2 absorption in aqueous hexamethylenediamine, Int. J. Greenhouse Gas Control 56 (2017) 116–125, https://doi.org/10.1016/j.ijggc.2016.11.023.

[10] P. Singh, W.P.M. van Swaaij, D.W.F. (Wim) Brilman, Kinetics study of carbon dioxide absorption in aqueous solutions of 1,6-hexamethyldiamine (HMDA) and 1,6-hexamethyldiamine, N,N′ di-methyl (HMDA, N,N′), Chem. Eng. Sci. 66 (2011) 4521–4532, https://doi.org/10.1016/j.ces.2011.06.008.

[11] B.K. Mondal, S.S. Bandyopadhyay, A.N. Samanta, Vapor-liquid equilibrium measurement and ENRTL modeling of CO_2 absorption in aqueous hexamethylenediamine, Fluid Phase Equilib. 402 (2015) 102–112, https://doi.org/10.1016/j.fluid.2015.05.033.

[12] P. Singh, D.W.F. (Wim) Brilman, M.J. Groeneveld, Evaluation of CO_2 solubility in potential aqueous amine-based solvents at low CO_2 partial pressure, Int. J. Greenhouse Gas Control 5 (2011) 61–68, https://doi.org/10.1016/j.ijggc.2010.06.009.

[13] G.F. Versteeg, W. Van Swaalj, Solubility and diffusivity of acid gases (carbon dioxide, nitrous oxide) in aqueous alkanolamine solutions, J. Chem. Eng. Data 33 (1988) 29–34, https://doi.org/10.1021/je00051a011.

[14] S.S. Laddha, J.M. Diaz, P.V. Danckwerts, The N_2O analogy: the solubilities of CO_2 and N_2O in aqueous solutions of organic compounds, Chem. Eng. Sci. 36 (1981) 228–229, https://doi.org/10.1016/0009-2509(81)80074-7.

[15] B.K. Mondal, S.S. Bandyopadhyay, A.N. Samanta, Kinetics of CO_2 absorption in aqueous hexamethylenediamine blended N-methyldiethanolamine, Ind. Eng. Chem. Res. 56 (2017) 14902–14913, https://doi.org/10.1021/acs.iecr.7b02744.

[16] J. Ying, D.A. Eimer, Determination and measurements of mass transfer kinetics of CO_2 in concentrated aqueous monoethanolamine solutions by a stirred cell, Ind. Eng. Chem. Res. 52 (2013) 2548–2559, https://doi.org/10.1021/ie303450u.

[17] B.K. Mondal, S.S. Bandyopadhyay, A.N. Samanta, Equilibrium solubility measurement and Kent-Eisenberg modeling of CO_2 absorption in aqueous mixture of N-methyldiethanolamine and hexamethylenediamine, Greenhouse Gases Sci. Technol. 7 (2017) 202–214, https://doi.org/10.1002/ghg.1653.

[18] B.K. Mondal, S.S. Bandyopadhyay, A.N. Samanta, Experimental measurement and Kent-Eisenberg modelling of CO_2 solubility in aqueous mixture of 2-amino-2-methyl-1-propanol and hexamethylenediamine, Fluid Phase Equilib. 437 (2017) 118–126, https://doi.org/10.1016/j.fluid.2017.01.020.

[19] M.K. Park, O.C. Sandall, Solubility of carbon dioxide and nitrous oxide in 50 mass % methyldiethanolamine, J. Chem. Eng. Data 46 (2001) 166–168, https://doi.org/10.1021/je000190t.

[20] P.M.M. Blauwhoff, G.F. Versteeg, W.P.M. Van Swaaij, A study on the reaction between CO_2 and alkanolamines in aqueous solutions, Chem. Eng. Sci. 38 (1983) 1411–1429, https://doi.org/10.1016/0009-2509(83)80077-3.

[21] J. Van Holst, G.F. Versteeg, D.W.F. Brilman, J.A. Hogendoorn, Kinetic study of CO_2 with various amino acid salts in aqueous solution, Chem. Eng. Sci. 64 (2009) 59–68, https://doi.org/10.1016/j.ces.2008.09.015.

[22] S. Mazinani, A. Samsami, A. Jahanmiri, A. Sardarian, Solubility (at Low Partial Pressures), density, viscosity, and corrosion rate of carbon dioxide in blend solutions of monoethanolamine (MEA) and sodium glycinate (SG), J. Chem. Eng. Data 56 (2011) 3163–3168, https://doi.org/10.1021/je2002418.

[23] M. Xiao, H. Liu, R. Idem, P. Tontiwachwuthikul, Z. Liang, A study of structure – activity relationships of commercial tertiary amines for post-combustion CO_2 capture, Appl. Energy. 184 (2016) 219–229, https://doi.org/10.1016/j.apenergy.2016.10.006.

[24] H. Suleman, A.S. Maulud, Z. Man, Review and selection criteria of classical thermodynamic models for acid gas absorption in aqueous alkanolamines, Rev. Chem. Eng. 31 (2015) 599–639, https://doi.org/10.1515/revce-2015-0030.

[25] M.-H. Li, K.-P. Shen, Calculation of equilibrium solubility of carbon dioxide in aqueous mixtures of monoethanolamine with methyldiethanolamine, Fluid Phase Equilib. 85 (1993) 129–140, https://doi.org/10.1016/0378-3812(93)80008-B.

[26] S. Shen, Y. Zhao, Y. Bian, Y. Wang, H. Guo, H. Li, CO_2 absorption using aqueous potassium lysinate solutions: vapor – liquid equilibrium data and modelling, J. Chem. Thermodyn. 115 (2017) 209–220, https://doi.org/10.1016/j.jct.2017.07.041.

[27] M.Z. Haji-Sulaiman, M.K. Aroua, A. Benamor, Analysis of equilibrium data of CO_2 in aqueous solutions of diethanolamine (DEA), methyldiethanolamine (MDEA) and their mixtures using the modified Kent Eisenberg model, Chem. Eng. Res. Des. 76 (1998) 961–968, https://doi.org/10.1205/026387698525603.

[28] D.H. Everett, B.R.W. Pinsent, The dissociation constants of ethylene diammonium and hexamethylene diammonium ions from 0 degrees to 60 degrees C, Proc. R. Soc. A Math. Phys. Eng. Sci. 215 (1952) 416–429, https://doi.org/10.1098/rspa.1952.0221.

[29] A.F. Portugal, J.M. Sousa, F.D. Magalhães, A. Mendes, Solubility of carbon dioxide in aqueous solutions of amino acid salts, Chem. Eng. Sci. 64 (2009) 1993–2002, https://doi.org/10.1016/j.ces.2009.01.036.

[30] Y.-H. Hsu, R.B. Leron, M.-H. Li, Solubility of carbon dioxide in aqueous mixtures of (reline + monoethanolamine) at T = (313.2 to 353.2)K, J. Chem. Thermodyn. 72 (2014) 94–99, https://doi.org/10.1016/j.jct.2014.01.011.

[31] S.-W. Park, Y. Son, D. Park, K.-J. Oh, Absorption of carbon dioxide into aqueous solution of sodium glycinate, Sep. Sci. Technol. 43 (2008) 3003–3019, https://doi.org/10.1080/01496390802219620.

[32] A.F. Portugal, P.W.J. Derks, G.F. Versteeg, F.D. Magalhães, A. Mendes, Characterization of potassium glycinate for carbon dioxide absorption purposes, Chem. Eng. Sci. 62 (2007) 6534–6547, https://doi.org/10.1016/j.ces.2007.07.068.

[33] P.D. Vaidya, P. Konduru, M. Vaidyanathan, E.Y. Kenig, Kinetics of carbon dioxide removal by aqueous alkaline amino acid salts, Ind. Eng. Chem. Res. 49 (2010) 11067–11072, https://doi.org/10.1021/ie100224f.

[34] B.R.W. Pinsent, L. Pearson, F.J.W. Roughton, The kinetics of combination of carbon dioxide with hydroxide ions, Trans. Faraday Soc. 52 (1956) 1512, https://doi.org/10.1039/tf9565201512.